Theoretical prediction of residual stresses induced by cold spray with experimental validation

Boruah, D., Zhang, X. & Doré, M.

Original citation & hyperlink:
Boruah, D, Zhang, X & Doré, M 2019, 'Theoretical prediction of residual stresses induced by cold spray with experimental validation', Multidiscipline Modeling in Materials and Structures, vol. 15, no. 3, pp. 599-616.
https://dx.doi.org/10.1108/MMMS-08-2018-0150

DOI 10.1108/MMMS-08-2018-0150
ISSN 1573-6105
ESSN 1573-6113

Publisher: Emerald

Theoretical prediction of residual stresses induced by cold spray with experimental validation

Dibakor Boruah [a,b, 1], Xiang Zhang [b, 2], Matthew Doré [c, 3]

[a] *National Structural Integrity Research Centre (NSIRC), TWI Ltd, Granta Park, Great Abington, Cambridge, United Kingdom, CB21 6AL*
[b] *Faculty of Engineering, Environment and Computing, Coventry University, Priory Street, Coventry, United Kingdom, CV1 5FB*
[c] *Integrity Management Group, TWI Ltd, Granta Park, Great Abington, Cambridge, United Kingdom, CB21 6AL*
[1] boruahd@uni.coventry.ac.uk, [2] xiang.zhang@coventry.ac.uk, [3] matthew.dore@twi.co.uk

Abstract

Purpose- This study aims to develop a simple analytical model for predicting the through-thickness distribution of residual stresses in a cold spray deposit-substrate assembly.

Design/methodology/approach- Layer by layer build up of residual stresses induced by both the peening dominant and thermal mismatch dominant cold spray processes, taking into account the force and moment equilibrium requirements. The proposed model has been validated with the neutron diffraction measurements, taken from the published literature for different combinations of deposit-substrate assemblies comprising Cu, Mg, Ti, Al and Al alloys.

Findings- Through a parametric study, the influence of geometrical variables (number of layers, substrate height and individual layer height) on the through-thickness residual stress distribution and magnitude are elucidated. Both the number of deposited layers and substrate height affect residual stress magnitude, whereas the individual layer height has little effect. A good agreement has been achieved between the experimentally measured stress distributions and predictions by the proposed model.

Originality/value-

The proposed model provides a more thorough explanation of residual stress development mechanisms by the cold spray process along with mathematical representation. Comparing to existing analytical and finite element methods, it provides a quicker estimation of the residual stress distribution and magnitude. This paper provides comparisons and contrast of the two different residual stress mechanisms: the peening dominant and the thermal mismatch dominant. The proposed model allows parametric studies of geometric variables, and can potentially contribute to cold spray process optimisation aiming at residual stress control.

Keywords: Additive manufacturing, Analytical modelling, Coatings, Cold spray, Repairs, Residual stress, Theoretical prediction, Thermal spray

Nomenclature

a_n , b_n	Constants (related to material's properties, cold spray (CS) process parameters, and specimen geometry)
h, Δh	Substrate height, CS layer height, respectively (mm)
k	Residual stress in a newly deposited CS layer or the near-surface residual stress (MPa)
m	An individual CS deposited layer, m = $1, 2, 3, 4, \ldots\ldots\ldots (n-1)$
n	Number of CS deposited layers $(1, 2, 3, 4, \ldots\ldots\ldots$ n)
y	Distance from the bottom surface of the substrate (mm)
$\Delta\sigma_n(y)$	Stress increment in the substrate due to deposition of the n^{th} CS layer (MPa)
$\Delta\sigma_{TS_{(nL)}}(y)$	Total (*T*) stress increment in the substrate (*S*) due to deposition of '*n*' CS layers (*nL*) (MPa)
$\Delta\sigma_{T(Lm)_{(Ln)}}(y)$	Total (*T*) stress increment in m^{th} layer (Lm) due to deposition of the n^{th} CS layer (Ln) (MPa)

1 Introduction

Cold spray (CS) is an increasingly used solid-state additive material deposition technique of high strain-rate, where powder particles are propelled to reach a critical velocity by a supersonic jet of preheated compressed He or N_2 gas. The high-velocity impact of the powder particles and their associated severe plastic deformation, results in a coating on the substrate or previously deposited particles. The three major applications of the CS process are protective coating, repair of high-value metallic components, and additive manufacturing [1,2]. The build-up of residual stresses during the CS deposition process plays a significant role in the development of a compact and well adherent coating or coatings suitable for repair applications. The distribution and the magnitude of residual stresses influence the bonding mechanism, mechanical properties of the deposited materials, substrate-coating adhesion, and cohesion between deposited layers [3]. Therefore, it is very important to understand, predict and effectively control residual stresses in a CS deposit-substrate system, in order to optimise the integrity of a coating or repair, in terms of adhesion, wear, fatigue life, resistance to cracking and the overall in-service performance.

There are three approaches to evaluate residual stresses in engineering components, which are the analytical/empirical, numerical, and experimental methods. Even though the experimental methods possess various advantages, modelling of residual stresses is an attractive alternative method as it is quicker, inexpensive, and allows parametric studies. Many researchers have used analytical methods [3–11], and numerical models [3,8,11–19] for predicting residual stresses induced by the CS process.

Most of the current analytical models are based on the bending deformation method (also known as the deflection method or curvature method) [3–11], originally developed for evaluating residual stresses in thin coatings (e.g. thermal spray coatings, electrolysis film deposits) or shot-peened parts. In these methods, residual stresses were estimated from spraying or peening induced bending based on the relationship between the induced stresses and the magnitude of bending. Curvature based approaches are generally used for residual stress evaluation on narrow strips (suitable only for thin coatings with a few layers) to avoid multi-axial curvature and mechanical instability [20]. Also, the elastic modulus should be determined experimentally in order to achieve better evaluation [4,7,20]. The latest version of this method is known as the in-situ curvature method or continuous curvature measurement method for determining the through-thickness stress profiles by continuous monitoring the curvature and temperature changes during the deposition process, albeit some numerical and experimental challenges [5,7]. The main drawbacks of this method are: (i) it is impossible to retrace stresses in the specimens without recorded in-situ deflection and thermal history, and (ii) it works only for certain design and geometries [5]. Many researchers [3,5,6,11,21] have used an analytical model [22] for predicting the through thickness residual stress distribution in CS deposit-substrate assemblies. However, this method is very complicated as it involves more experimental measurements, such as Young's modulus (both for the deposited and substrate material) and induced curvature changes (before deposition, after each successive layer deposition, and the final deposit-substrate composite after cooling down to room temperature). It also requires calculations for evaluating effective Young's modulus, effective stiffness in-plane stress condition and neutral axis position, etc., in order to calculate stresses at the mid-point of each layer and at the top and bottom of the substrate [22].

Analytical methods based on the Hertzian contact and Taylor's impact test were originally developed for predicting shot peening induced residual stresses. Methods based on Hertzian contact can be used to measure the maximum residual stress at the free surface of the deposits, and is strongly dependent on the elasto-plastic properties of the material (mainly on the yield strength) and spray kinetic conditions. Limitations of this method are stated in [5,6]. Taylor's impact test can be used to measure the average strain rate and average impact pressure using estimated values of particle velocity, impact strain and impact duration [5,6]. Nevertheless, approaches based on the Hertzian contact and Taylor's impact are not suitable for predicting through-thickness residual stress profiles induced by the CS process. Therefore, these analytical methods are not suitable for evaluating through thickness distribution of residual stresses induced by thicker cold spray deposits.

Numerical methods are highly complicated, need large computational time and expertise in various physics-based theories and modelling techniques (e.g. fluid-dynamics, smoothed particle hydrodynamics, Gruneisen formulation, Lagrangian based finite element techniques, kinematic hardening models, thermo-mechanical modelling, high strain rate plasticity models, etc.) [3,8,11–18]. Moreover, the number of particles used in numerical models were limited, as the particle to substrate and particle to particle interactions were defined manually due to unavailability of user subroutines to define these interactions. Increasing the number of particles leads to an increase in particle interactions exponentially, resulting in manual modelling setup impracticable [17].

Therefore, it is of great interest to develop a simple and efficient analytical model to predict residual stress distribution and magnitude induced by the CS process. This study aims to develop an analytical model based on a generalised concept of the force and moment equilibrium requirements within a system. This model demonstrates the distribution and magnitude of residual stresses in the substrate as well as previously deposited layers due to the stress induced by a newly deposited CS layer. The original idea of the analytical model is based on the work of Shiomi [23], which has demonstrated the increment of residual stresses due to the deposition of additive layers in the Selective Laser Melting (SLM) process. In the present study, Shiomi's idea is further developed and modified with changes in the assumptions, for predicting of residual stresses arising from the CS processes.

2 Formulation of the proposed model

2.1 Mechanisms

In view of residual stress generation, CS processes can be categorised into two different mechanisms: (i) Peening dominant CS process, where plastic deformation is caused by the peening impact of high-velocity powder particles. In this process, peening stresses are dominant due to its low deposition temperature and high velocity of the particles resulting in reduced thermal input and increased peening effect [8–10]. For example: Cu/Cu, Cu/Al, Al/Al, Al/Cu [5], Al/Mg, Al6061/Mg, Al7075/Mg [6]. (ii) Thermal mismatch dominant CS process, which is originated from quenching of the sprayed splats, owing to the different thermal contraction of the substrate and deposited material, and/or temperature gradient in multi-pass deposition process [6–8,10]. For example: Ti/Cu [21], Al/Mg [6].

In the peening dominant processes, stresses near the free surface of CS deposits are generally compressive in nature, and gradually become tensile at the interface. Then, there is a discontinuity in the stress magnitude or the slope on either side of the interface due to the stiffness difference arising from the difference in the elastic modulus between the substrate and CS deposits [21,24]. Therefore, process induced residual strains are continuous at the interface,

but stress values are different on either side of the interface. Further, from the interface, stresses gradually changes to compressive towards the bottom of the substrate. As an example, Fig. 1(a) shows a residual stress profile for Al 6061 coatings on Mg substrate, using the Cold Gas Technology (CGT) system [6].

In the thermal mismatch dominant process, stresses at the free surface of CS deposits can be tensile [6,21] or neutral [21], depending on the spray process parameters and material properties [7]; then stresses gradually become compressive in the interface region. For the substrate material, stress distribution is similar to peening dominant CS processes. Fig 1(b) shows an example stress profile for Ti coatings on Cu substrate, using the CGT system [21].

Based on the experimentally measured residual stress distribution [3,5,6,21], a conceptual model has been developed to interpret the mechanism of residual stress build up in the peening dominant CS deposition process, as illustrated in Fig. 2(a) and 2(b). Figure 2(a) shows the generation of a downward bending moment (M_1) in the CS deposit-substrate assembly by a pair of equal and opposite forces to balance the compressive residual stress (k) induced by the peening impact of the spraying particles after depositing the 1st layer. This process gets more complicated as more layers build up and coating height becomes influential with respect to the given substrate height. Each successive CS layer induces the same amount of misfit strain each time on a deposit-substrate of increasing height, due to the peening impact of the powder particle. Therefore, the final stress distribution in a multilayer deposit-substrate assembly is significantly different from the initial system with a single layer, which can be determined by a succession of force and moment balance calculations. Fig 2 (b) represents the final state of residual stress distribution in a deposit-substrate assembly after deposition of 'n' layers, having a negative moment in the substrate and a positive moment in the coating to satisfy the force and moment equilibrium requirements. As a result, residual stresses near the free surface of the deposits and substrate are compressive in nature, whereas residual stresses are tensile in nature at the interface to maintain equilibrium.

Similarly, in the case of thermal mismatch dominant CS process, mechanism of residual stress build up is illustrated in Fig. 2(c) and 2(d). Figure 2(c) shows the generation of a negative bending moment (M_1) in the CS deposit-substrate assembly by a pair of equal and opposite forces to balance the process induced tensile residual stress (k) induced after depositing the 1st layer. Each successive CS layer induces the same amount of thermal misfit strain (which may be due to quenching, thermal gradient, and/or differences in the coefficient of thermal expansion) each time on a deposit-substrate system of increasing height. Fig 2 (d) represents the final state of residual stress distribution in a deposit-substrate assembly after deposition of 'n' layers, having a negative moment both in the substrate and CS coating. As a result, residual

stresses at the free surface of the deposits and in the substrate just below the interface are tensile in nature, whereas residual stresses are compressive in the coating region just above the interface and bottom of the substrate.

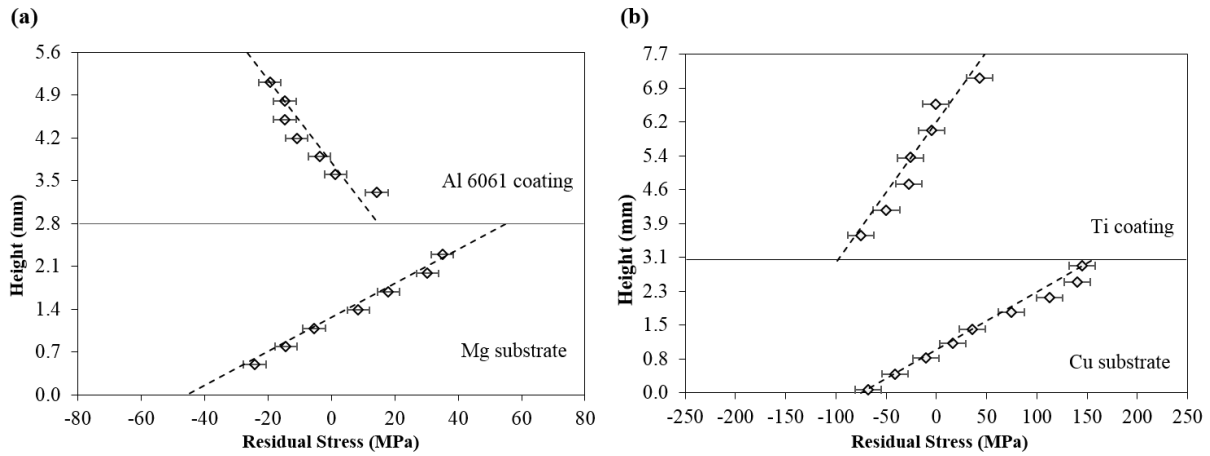

Figure 1: Typical residual stress profiles measured by neutron diffraction: (a) peening dominant cold spray (CS) process: CGT Al6061/Mg [6], (b) thermal mismatch dominant CS process: CGT Ti/Cu [21].

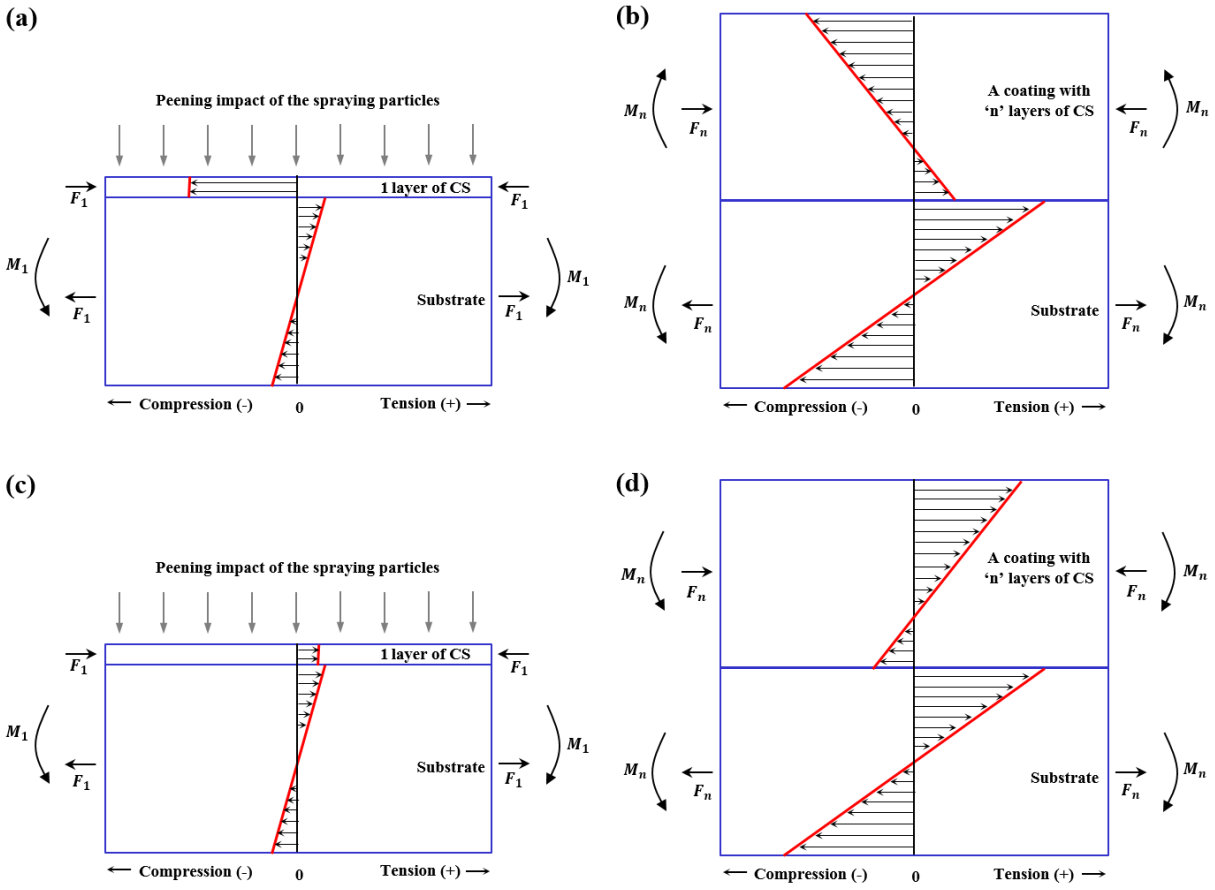

Figure 2: Conceptual model showing the mechanism of residual stress build up during CS processes and stress distribution; left: after deposition of the 1st layer; right: after deposition of '*n*' layers. Here, (a) and (b) represent the peening dominant CS process; (c) and (d) shows the thermal mismatch dominant CS process.

2.2 Assumptions

Based on the experimental observation and the aforementioned conceptual model, the following assumptions were made for the proposed analytical model:

1) The substrate is free from residual stresses prior to material deposition and fixed in position by a sample holder which allows distortion (if any) during the deposition process.
2) The general beam theory is valid, and no external forces are applied to the deposit-substrate assembly.
3) The substrate and CS deposited layers have the same width and same length.
4) Residual stress in each newly deposited CS layer has the same value 'k', which is a constant throughout the layer height (Δh).
5) The height of each newly CS deposited layer is the same, i.e. 'Δh'.
6) Linear stress distribution in the substrate can be described by a linear equation (Section 2.3) following an increment of residual stress '$\Delta\sigma$' owing to deposition of a new CS layer.

2.3 Formulations

2.3.1 Peening dominant CS process

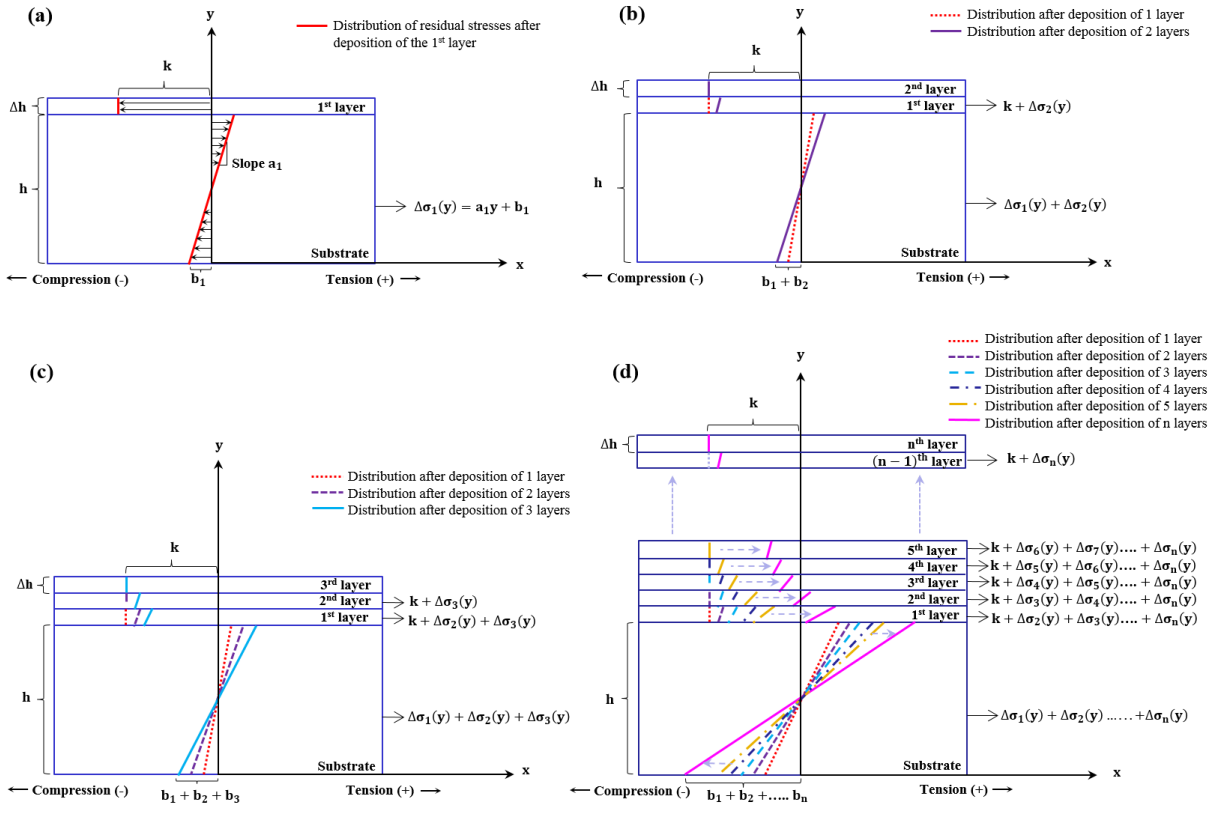

Figure 3: Build up of residual stresses by peening dominant CS process: residual stress distribution due to the stress induced by deposition of (a) one layer, (b) two layers, (c) three layers, and (d) 'n' layers.

Fig. 3 shows the build up of residual stresses in the substrate and CS deposits due to the deposition of the first, second, and n^{th} layer, respectively, for the peening dominant CS process.

A summary of the key equations of the proposed analytical formulation are presented below from eq. (1) to eq. (6).

It is assumed that stress increment distributes linearly in the substrate due to the deposition of $1^{st}, 2^{nd}, \dots\dots\dots n^{th}$ layer of CS respectively as follows:

$$\left.\begin{aligned}
&\Delta\sigma_1(y) = a_1 y + b_1\\
&\Delta\sigma_2(y) = a_2 y + b_2\\
&\dots\dots\dots\dots\dots\dots\dots\dots\\
&\Delta\sigma_n(y) = a_n y + b_n
\end{aligned}\right\} \quad (1)$$

After solving the force and moment equilibrium equations, we can get (see Appendix I) -

$$\left.\begin{aligned}
&a_1 = -\frac{6k\Delta h(h+\Delta h)}{h^3},\ b_1 = \frac{k\Delta h(2h+3\Delta h)}{h^2}\\
&a_2 = -\frac{6k\Delta h(h+2\Delta h)}{(h+\Delta h)^3},\ b_2 = \frac{k\Delta h(2h+5\Delta h)}{(h+\Delta h)^2}\\
&\dots\dots\dots\dots\dots\dots\dots\dots\dots\dots\dots\dots\dots\dots\dots\dots\dots\dots\dots\dots\dots\dots\dots\dots\\
&a_n = -\frac{6k\Delta h(h+n\Delta h)}{\{h+(n-1)\Delta h\}^3},\ b_n = \frac{k\Delta h\{2h+(2n+1)\Delta h\}}{\{h+(n-1)\Delta h\}^2}
\end{aligned}\right\} \quad (2)$$

Using the values of $(a_1, b_1), (a_2, b_2), \dots\dots (a_n, b_n)$, the total stress increment in the substrate due to the deposition of $1, 2, \dots\dots n$ layers, respectively, can be expressed by eq. (3):

$$\left.\begin{aligned}
&\Delta\sigma_{TS_{(1L)}}(y) = -6k\Delta h y\left(\frac{h+\Delta h}{h^3}\right) + k\Delta h\left(\frac{2h+3\Delta h}{h^2}\right)\\
&\Delta\sigma_{TS_{(2L)}}(y) = -6ky\Delta h\left\{\frac{h+\Delta h}{h^3} + \frac{h+2\Delta h}{(h+\Delta h)^3}\right\} + k\Delta h\left\{\frac{2h+3\Delta h}{h^2} + \frac{2h+5\Delta h}{(h+\Delta h)^2}\right\}\\
&\dots\dots\dots\dots\dots\dots\dots\dots\dots\dots\dots\dots\dots\dots\dots\dots\dots\dots\dots\dots\dots\dots\dots\dots\dots\dots\dots\dots\dots\dots\dots\dots\dots\dots\dots\dots\\
&\Delta\sigma_{TS_{(nL)}}(y) = -6ky\Delta h\left\{\frac{h+\Delta h}{h^3} + \frac{h+2\Delta h}{(h+\Delta h)^3} + \frac{h+3\Delta h}{(h+2\Delta h)^3} \dots\dots\dots + \frac{h+n\Delta h}{\{h+(n-1)\Delta h\}^3}\right\} +\\
&\qquad k\Delta h\left\{\frac{2h+3\Delta h}{h^2} + \frac{2h+5\Delta h}{(h+\Delta h)^2} + \frac{2h+7\Delta h}{(h+2\Delta h)^2} \dots\dots\dots + \frac{2h+(2n+1)\Delta h}{\{h+(n-1)\Delta h\}^2}\right\}
\end{aligned}\right\} \quad (3)$$

Therefore, the total increment of residual stresses in the substrate due to the deposition of 'n' layers of CS can be expressed by a simplified eq. (4):

$$\Delta\sigma_{TS_{(nL)}}(y) = -6ky\Delta h\sum_{n=1}^{n}\left\{\frac{h+n\Delta h}{\{h+(n-1)\Delta h\}^3}\right\} + k\Delta h\sum_{n=1}^{n}\left\{\frac{2h+(2n+1)\Delta h}{\{h+(n-1)\Delta h\}^2}\right\} \quad (4)$$

The total stress increment in the $1^{st}, 2^{nd}, \dots\dots\dots (n-1)^{th}$ layers respectively due to the deposition of the n^{th} layer of CS can be expressed by eq. (5):

$$\left.\begin{aligned}
&\Delta\sigma_{TL1_{(Ln)}}(y) = k - 6ky\Delta h\left\{\frac{h+2\Delta h}{(h+\Delta h)^3} + \frac{h+3\Delta h}{(h+2\Delta h)^3} \dots\dots\dots + \frac{h+n\Delta h}{\{h+(n-1)\Delta h\}^3}\right\} +\\
&\qquad k\Delta h\left\{\frac{2h+5\Delta h}{(h+\Delta h)^2} + \frac{2h+7\Delta h}{(h+2\Delta h)^2} \dots\dots\dots + \frac{2h+(2n+1)\Delta h}{\{h+(n-1)\Delta h\}^2}\right\}\\
&\Delta\sigma_{TL2_{(Ln)}}(y) = k - 6ky\Delta h\left\{\frac{h+3\Delta h}{(h+2\Delta h)^3} + \frac{t+4\Delta t}{(t+3\Delta t)^3} \dots\dots\dots + \frac{h+n\Delta h}{\{h+(n-1)\Delta h\}^3}\right\} +\\
&\qquad k\Delta h\left\{\frac{2h+7\Delta h}{(h+2\Delta h)^2} + \frac{2h+9\Delta h}{(h+3\Delta h)^2} \dots\dots\dots + \frac{2h+(2n+1)\Delta h}{\{h+(n-1)\Delta h\}^2}\right\}\\
&\dots\dots\dots\dots\dots\dots\dots\dots\dots\dots\dots\dots\dots\dots\dots\dots\dots\dots\dots\dots\dots\dots\dots\dots\dots\dots\dots\dots\dots\dots\dots\dots\dots\dots\dots\dots\\
&\Delta\sigma_{T\{L(n-1)\}_{(Ln)}}(y) = k - 6ky\Delta h\left\{\frac{(h+n\Delta h)}{\{h+(n-1)\Delta h\}^3}\right\} + k\Delta h\left\{\frac{2h+(2n+1)\Delta h}{\{(h+(n-1)\Delta h)\}^2}\right\}
\end{aligned}\right\} \quad (5)$$

Eq. (5) can be written in a simplified form as eq. (6):

$$\Delta\sigma_{T(Lm)_{(Ln)}}(y) = k - 6ky\Delta h\sum_{m+1}^{n}\left\{\frac{h+n\Delta h}{\{h+(n-1)\Delta h\}^3}\right\} + k\Delta h\sum_{m+1}^{n}\left\{\frac{2h+(2n+1)\Delta h}{\{h+(n-1)\Delta h\}^2}\right\} \quad (6)$$

Equations (4) and (6) can be used to calculate the distribution and magnitude of residual stresses in a CS deposit-substrate assembly if the residual stress in a newly deposited layer (i.e. 'k') is known. The value of 'k' relies on the material's properties (particularly the yield strength), CS process parameters, and the specimen geometry; which can be evaluated by measuring the near-surface residual stress using the incremental hole drilling or X-ray diffraction method.

2.3.2 Thermal mismatch dominant CS process

Fig. 4 shows the build up of residual stresses in the substrate and CS deposits due to the deposition of the first, second, and n^{th} layer respectively, for the thermal mismatch dominant CS process. A summary of the key equations are presented below.

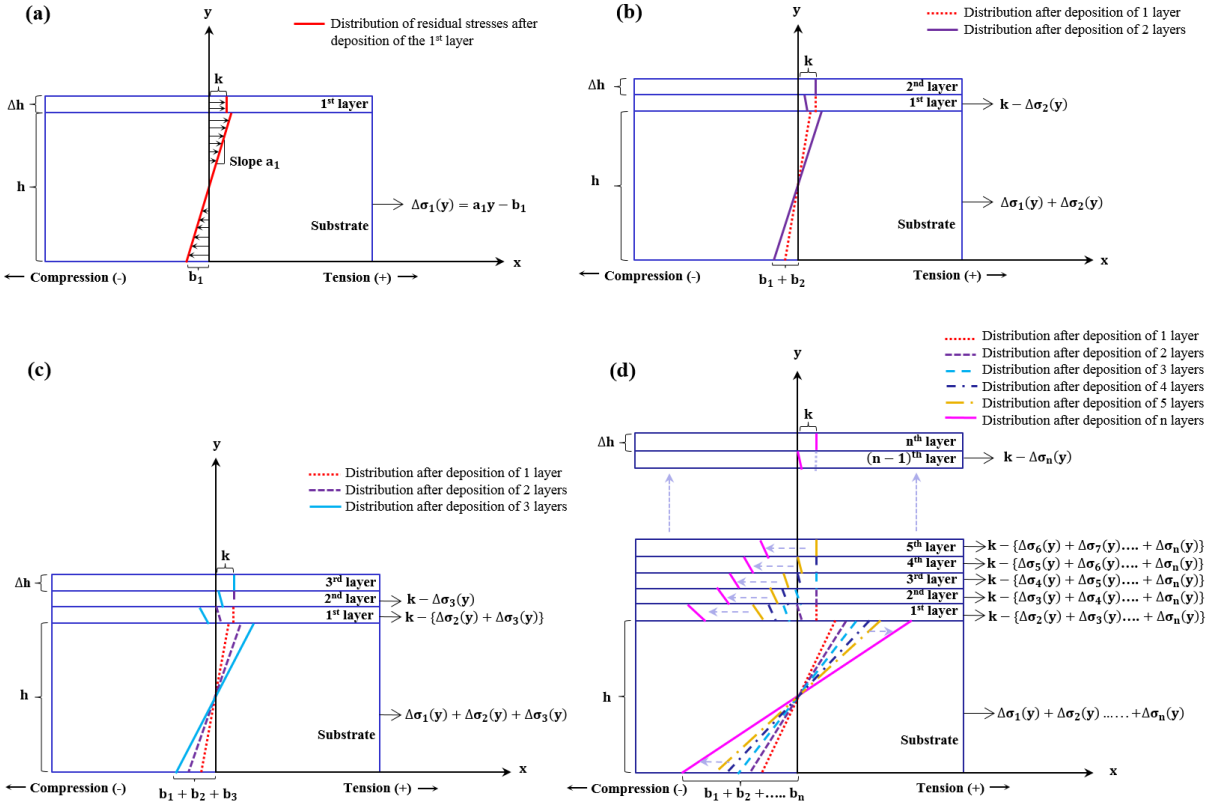

Figure 4: Build up of residual stresses by thermal mismatch dominant CS process: residual stress distribution due to the stress induced by deposition of (a) one layer, (b) two layers, (c) three layers, and (d) 'n' layers.

It is assumed that stress increment distributes linearly in the substrate due to the deposition of the $1^{st}, 2^{nd}, \ldots\ldots\ldots n^{th}$ CS layer respectively as follows:

$$\left.\begin{aligned}&\Delta\sigma_1(y) = a_1y - b_1\\&\Delta\sigma_2(y) = a_2y - b_2\\&\ldots\ldots\ldots\ldots\ldots\ldots\ldots\\&\Delta\sigma_n(y) = a_ny - b_n\end{aligned}\right\} \quad (7)$$

After solving the force and moment balance equations:

$$
\left.
\begin{aligned}
&a_1 = \frac{6k\Delta h(h+\Delta h)}{h^3},\ b_1 = -\frac{k\Delta h(2h+3\Delta h)}{h^2} \\
&a_2 = \frac{6k\Delta h(h+2\Delta h)}{(h+\Delta h)^3},\ b_2 = -\frac{k\Delta h(2h+5\Delta h)}{(h+\Delta h)^2} \\
&\ldots\ldots\ldots\ldots\ldots\ldots\ldots\ldots\ldots\ldots\ldots\ldots \\
&a_n = \frac{6k\Delta h(h+n\Delta h)}{\{h+(n-1)\Delta h\}^3},\ b_n = -\frac{k\Delta h\{2h+(2n+1)\Delta h\}}{\{h+(n-1)\Delta h\}^2}
\end{aligned}
\right\} \quad (8)
$$

Using the values of $(a_1, b_1), (a_2, b_2), \ldots\ldots\ldots (a_n, b_n)$ from eq. (8), the total stress increment in the substrate due to the deposition of $1, 2, \ldots\ldots\ldots n$ layers, respectively, can be expressed by eq. (9):

$$
\left.
\begin{aligned}
&\Delta\sigma_{TS_{(1L)}}(y) = 6k\Delta hy\left(\frac{h+\Delta h}{h^3}\right) - k\Delta h\left(\frac{2h+3\Delta h}{h^2}\right) \\
&\Delta\sigma_{TS_{(2L)}}(y) = 6ky\Delta h\left\{\frac{h+\Delta h}{h^3} + \frac{h+2\Delta h}{(h+\Delta h)^3}\right\} - k\Delta h\left\{\frac{2h+3\Delta h}{h^2} + \frac{2h+5\Delta h}{(h+\Delta h)^2}\right\} \\
&\ldots\ldots\ldots\ldots\ldots\ldots\ldots\ldots\ldots\ldots\ldots\ldots\ldots\ldots\ldots\ldots\ldots\ldots\ldots\ldots \\
&\Delta\sigma_{TS_{(nL)}}(y) = 6ky\Delta h\left\{\frac{h+\Delta h}{h^3} + \frac{h+2\Delta h}{(h+\Delta h)^3} + \frac{h+3\Delta h}{(h+2\Delta h)^3} \ldots\ldots\ldots + \frac{h+n\Delta h}{\{h+(n-1)\Delta h\}^3}\right\} - \\
&\qquad k\Delta h\left\{\frac{2h+3\Delta h}{h^2} + \frac{2h+5\Delta h}{(h+\Delta h)^2} + \frac{2h+7\Delta h}{(h+2\Delta h)^2} \ldots\ldots\ldots + \frac{2h+(2n+1)\Delta h}{\{h+(n-1)\Delta h\}^2}\right\}
\end{aligned}
\right\} \quad (9)
$$

Therefore, the total increment of residual stresses in the substrate due to the deposition of 'n' layers of CS can be expressed by a simplified eq. (10):

$$\Delta\sigma_{TS_{(nL)}}(y) = 6ky\Delta h\sum_{n=1}^{n}\left\{\frac{h+n\Delta h}{\{h+(n-1)\Delta h\}^3}\right\} - k\Delta h\sum_{n=1}^{n}\left\{\frac{2h+(2n+1)\Delta h}{\{h+(n-1)\Delta h\}^2}\right\} \quad (10)$$

The total stress increment in the $1^{st}, 2^{nd}, 3^{rd}, \ldots\ldots\ldots (n-1)^{th}$ layers respectively due to the deposition of the n^{th} layer of CS were derived as per the figure 4 (similar to the derivation for eq. 5 and eq. 6). It was found that stress distribution in the CS layers for the thermal mismatch dominant process can be expressed by the same equation as eq. (6). Therefore, in the case of thermal mismatch dominant CS process, eqs. (10) and (6) can be used to calculate the distribution and magnitude of residual stresses in the substrate and CS deposits, respectively.

3 Parametric study of geometrical variables

A parametric study has been performed in terms of the influence of the deposited layer number, substrate height, and individual layer height on the distribution and magnitude of residual stresses in a CS deposit-substrate assembly. The parametric study presented here is to understand the effect of geometrical variables on residual stresses for both the peening dominant and thermal mismatch dominant CS processes, which is not material specific. For the peening dominant CS process, the value of *'k'* is assumed as -50 MPa, which is within the range of 'k' values (-7.8 to -80.6 MPa) for peening dormant process according to [3,5,6]. For the thermal misfit dominant CS process, 'k' is set as 45 MPa, which is within the range of 'k' values (~10.0 to 48.5 MPa) for thermal mismatch dominant CS process according to [6,21].

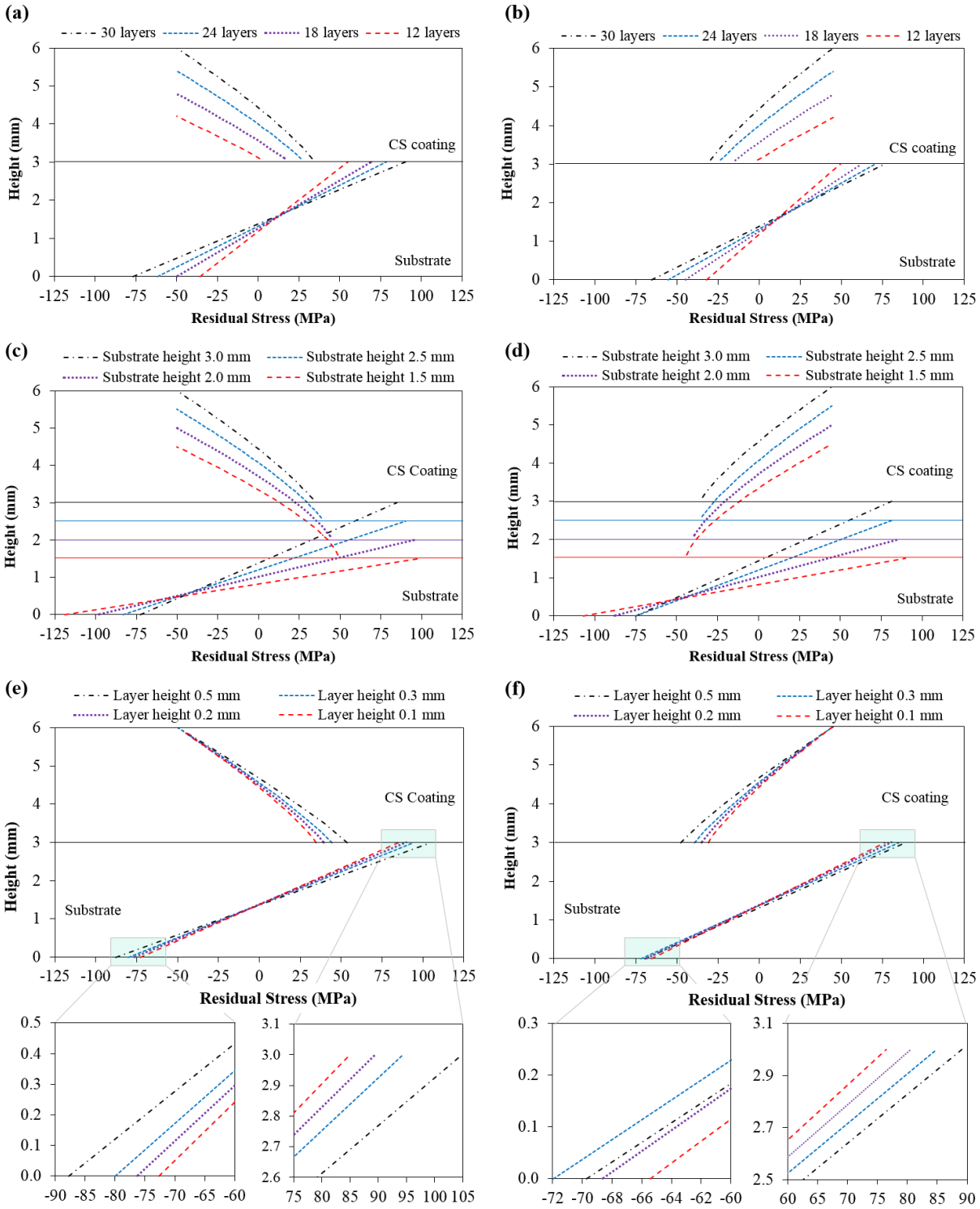

Figure 5: Distribution of residual stresses with the variation of number of layers in (a) and (b), substrate height in (c) and (d), and individual layer height in (e) and (f). The peening dominant CS process is presented in (a), (c) and (e); the thermal mismatch dominant CS process is presented in (b), (d) and (f).

Residual stresses arising from the peening dominant CS process are represented in Figs. 5(a), (c) and (e), and from the thermal mismatch dominant CS process in Figs. 5(b), (d) and (f). First, the effects of number of deposited layers are shown in Figs. 5(a) and (b). Four different cases were studied with the total number of CS layers being 12, 18, 24, and 30 respectively, keeping the individual layer height 0.1 mm and the substrate height 3 mm. It was found that the larger

the number of deposited layers, the higher the resulting residual stresses at the interface and at the bottom of the substrate. Fig. 5(c) and (d) show residual stress distribution due to the different substrate heights: 1.5 mm, 2.0 mm, 2.5 mm and 3.0 mm respectively, having CS layer height 0.1 mm and the total deposited material height 3 mm for all cases. It was found that the lower the substrate height, the higher the magnitude of resulting stresses at the interface and the bottom of the substrate. Residual stress distributions due to the variation of individual layer height are shown in Figs. 5(e) and (f) with substrate height 3 mm. The total deposited material height was 3 mm with four different layer heights: 0.1 mm (30 layers), 0.2 mm (15 layers), 0.3 mm (10 layers) and 0.5 mm (6 layers), respectively. It was found that the higher the individual layer height, the greater the magnitude of tensile residual stresses at the interface, however, the differences are not significant.

4 Validation and verification

The proposed analytical model has been validated with published neutron diffraction measurements and verified with the Tsui and Clyne's model and a finite element model [3,5,6,21]. Validation and verification examples are presented for eight different cases having different combinations of deposit-substrate assemblies in terms of materials used (Mg, Cu, Ti, Al, and Al alloys) and also the geometries. Table 1 represents the parameters used for predicting residual stresses using the proposed model. In addition to Table 1, a collated data set from the literature are also presented in Table A1 in Appendix III. Residual stress value in the newly deposited layer was considered as the near-surface residual stress value from neutron diffraction measurements. The layer height was assumed within the range of 100 μm to 290 μm to comply with a total height of the CS deposits.

Table 1: Details of reference neutron diffraction measurements used for the validation of the proposed analytical model. CGT stands for Cold Gas Technology system (convergent-divergent barrel, supersonic nozzle), and KM for Kinetic Metallization system (convergent barrel, sonic nozzle).

Cases	Substrate/deposits	Assumed 'k' value (MPa)	Substrate height 'h' (mm)	Assumed layer height 'Δh' (μm)	Number of layers 'n'
(a)	KM Cu/Cu [5]	-41.00	3.1	175	12
(b)	KM Cu/Al [5]	-80.55	2.6	140	10
(c)	KM Al/Cu [5]	-7.76	3.1	100	20
(d)	CGT Al7075/Mg [6]	-69.00	2.8	100	20
(e)	CGT Al6061/Mg [6]	-26.56	2.8	200	14
(f)	KM Al6061-T6/Al6061 [3]	-9.50	2.6	250	10
(g)	KM Ti/Cu [21]	15.00	3.1	260	15
(h)	CGT Al/Mg [6]	10.00	3.1	290	10

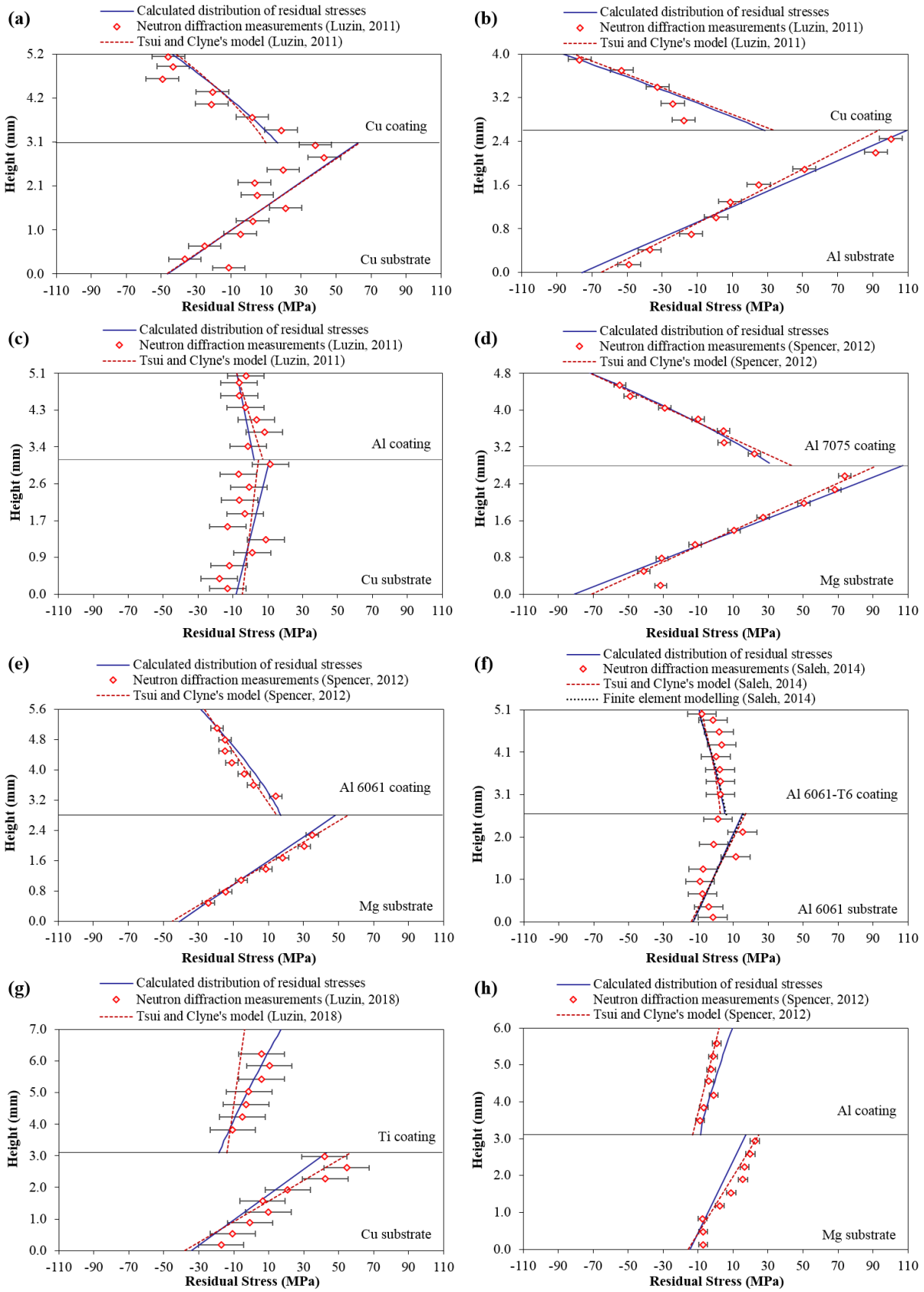

Figure 6: Comparison of calculated residual stress distributions with published experimental measurements: (a) KM Cu/Cu [5], (b) KM Cu/Al [5], (c) KM Al/Cu [5], (d) CGT Al7075/Mg [6], (e) CGT Al6061/Mg [6], (f) KM Al6061-T6/Al6061 [3], (g) KM Ti/Cu [21], (h) CGT Al/Mg [6].

Fig. 6 shows calculated residual stress distributions in this study and comparison with published experimental measurements. Figs. 6(a), (b), (c), (d), (e) and (f) represent the peening dominant CS process, whereas Figs. 6(g) and (h) show the thermal mismatch dominant CS process. From the Fig. 6, it can be observed that a good agreement has been achieved among the experimental stress distributions, existing analytical and numerical models' predictions, and the proposed model's predictions. Small differences between experimental and predicted values by this study could be due to the errors in the experimental measurements and/or the assumptions of the proposed model (such that it ignores the material's yielding, the interaction between the newly deposited layer and the substrate and/or previously deposited layers, etc.). Moreover, the experimental deposition may itself produce material inhomogeneity.

5 Conclusions

An analytical model was developed for predicting the distribution of residual stresses induced by the cold spray (CS) deposition process. The model is based on the force and moment equilibrium of the induced stresses by additive deposition of material layers. Based on the study, the following conclusions can be drawn:

1) A reasonably good agreement was achieved among the proposed model's predictions, published experimental measurements, and predictions by existing analytical and numerical models.
2) To calculate the through-thickness distribution of residual stresses in a cold spray deposit-substrate assembly, the proposed model requires only four parameters: the layer height, substrate height, number of deposited layers, and residual stress value in a newly deposited layer or the near-surface residual stress value.
3) Compared to existing analytical and finite element methods, this approach is simpler and can give a quick estimation of residual stress distribution and magnitude. With good calibration of residual stress value in a newly deposited layer, this analytical approach can be used to predict through-thickness residual stress profile in a cold spray deposit-substrate assembly with less cost and time.
4) The proposed model allows parametric studies of geometrical variables. Moreover, since the residual stress value in a newly deposited layer depends on the CS process parameters; therefore, with further experimental testing, the model can be linked with the CS process parameters, and can be used as an evaluation tool for the CS process parameter design aimed at residual stress control.

Acknowledgements

This publication was made possible by the sponsorship and support of the Lloyd's Register Foundation, which is a charitable organisation that helps to protect life and property by supporting engineering-related education, public engagement and the application of research.

References

[1] Jones R, Matthews N, Rodopoulos CA, Cairns K, Pitt S. On the use of supersonic particle deposition to restore the structural integrity of damaged aircraft structures. Int J Fatigue 2011;33:1257–67. doi:10.1016/j.ijfatigue.2011.03.013.

[2] Assadi H, Kreye H, Gärtner F, Klassen T. Cold spraying – A materials perspective. Acta Mater 2016;116:382–407. doi:10.1016/j.actamat.2016.06.034.

[3] Saleh M, Luzin V, Spencer K. Analysis of the residual stress and bonding mechanism in the cold spray technique using experimental and numerical methods. Surf Coatings Technol 2014;252:15–28. doi:10.1016/j.surfcoat.2014.04.059.

[4] Price TS, Shipway PH, McCartney DG. Effect of Cold Spray Deposition of a Titanium Coating on Fatigue Behavior of a Titanium Alloy. J Therm Spray Technol 2006;15:507–12. doi:10.1361/105996306X147108.

[5] Luzin V, Spencer K, Zhang MX. Residual stress and thermo-mechanical properties of cold spray metal coatings. Acta Mater 2011;59:1259–70. doi:10.1016/j.actamat.2010.10.058.

[6] Spencer K, Luzin V, Matthews N, Zhang MX. Residual stresses in cold spray Al coatings: The effect of alloying and of process parameters. Surf Coatings Technol 2012;206:4249–55. doi:10.1016/j.surfcoat.2012.04.034.

[7] Suhonen T, Varis T, Dosta S, Torrell M, Guilemany JM. Residual stress development in cold sprayed Al, Cu and Ti coatings. Acta Mater 2013;61:6329–37. doi:10.1016/j.actamat.2013.06.033.

[8] Arabgol Z, Assadi H, Schmidt T, Gartner F, Klassen T. Analysis of thermal history and residual stress in cold-sprayed coatings. J Therm Spray Technol 2014;23:84–90. doi:10.1007/s11666-013-9976-x.

[9] Bailly O, Laguionie T, Bianchi L, Vardelle M, Vardelle A. Residual stress measurements in cold sprayed tantalum coatings. Therm. Spray 2012 Proc. Int. Therm. Spray Conf., ASM International; 2012, p. 271–6.

[10] Rech S, Trentin A, Vezzù S, Legoux J-G, Irissou E, Arsenault B, et al. Characterization of residual stresses in Al and Al/Al2O3 cold sprayed coatings. Int. Therm. Spray Conf., ASM International; 2009, p. 1012–7.

[11] Benenati G, Lupoi R. Development of a deposition strategy in Cold Spray for Additive Manufacturing to minimize residual stresses. Procedia CIRP, vol. 55, 2016, p. 101–8. doi:10.1016/j.procir.2016.08.042.

[12] Shayegan G, Mahmoudi H, Ghelichi R, Villafuerte J, Wang J, Guagliano M, et al. Residual stress induced by cold spray coating of magnesium AZ31B extrusion. Mater Des 2014;60:72–84. doi:10.1016/j.matdes.2014.03.054.

[13] Xie J, Nelias D, Berre HW, Ito K, Ichikawa Y, Ogawa K. Numerical modeling for cold sprayed particle deposition. 40th Leeds-Lyon Symp. Tribol. Tribochemistry Forum, Sept. 4-6, 2013, Lyon, France: 2013.

[14] Phan T-D, Masood S, Jahedi M, Zahiri S. Residual stresses in cold spray process using finite element analysis. Mater Sci Forum 2010;654–656:1642–5. doi:10.4028/www.scientific.net/MSF.654-656.1642.

[15] Mahmoudi-Asl H. The effect of residual stress induced by cold spray coating on fatigue life of magnesium alloy, AZ31B. University of Waterloo, Waterloo, 2011.

[16] Ghelichi R, Bagherifard S, Macdonald D, Fernandez-Pariente I, Jodoin B, Guagliano M. Experimental and numerical study of residual stress evolution in cold spray coating. Appl Surf Sci 2014;288:26–33. doi:10.1016/j.apsusc.2013.09.074.
[17] Moonga KH, Jen T. Residual stress characterization from numerical analysis of the multi-particle impact behavior in cold spray. Proc. ASME 2017 Int. Mech. Eng. Congr. Expo., Tampa, Florida, USA: ASME; 2017, p. 1–10.
[18] Li W, Yang K, Zhang D, Zhou X. Residual stress analysis of cold-sprayed copper coatings by numerical simulation. J Therm Spray Technol 2016;25:131–42. doi:10.1007/s11666-015-0308-1.
[19] Song X, Everaerts J, Zhai W, Zheng H, Tan AWY, Sun W, et al. Residual stresses in single particle splat of metal cold spray process – Numerical simulation and direct measurement. Mater Lett 2018;230:152–6. doi:10.1016/j.matlet.2018.07.117.
[20] Withers PJ, Bhadeshia HKDH. Residual stress. Part 1 – Measurement techniques. Mater Sci Technol 2001;17:355–65. doi:10.1179/026708301101509980.
[21] Luzin V, Spencer K, Zhang M, Matthews N, Davis J, Saleh M. Residual Stresses in Cold Spray Coatings. In: Cavaliere P, editor. Cold -Spray Coatings, Cham: Springer; 2018, p. 451–80. doi:https://doi.org/10.1007/978-3-319-67183-3_16 451.
[22] Tsui YC, Clyne TW. An analytical model for predicting residual stresses in progressively deposited coatings Part 1: Planar geometry. Thin Solid Films 1997;306:23–33.
[23] Shiomi M, Osakadal K, Nakamural K, Yamashital T, Abe F. Residual stress within metallic model made by selective laser melting process. CIRP Ann - Manuf Technol 2004;53:195–8. doi:10.1016/S0007-8506(07)60677-5.
[24] Mercelis P, Kruth J. Residual stresses in selective laser sintering and selective laser melting. Rapid Prototyp J 2006;12:254–65. doi:10.1108/13552540610707013.

Appendix

I. Mathematical derivations for peening dominant cold spray process

(a) Deposition of the first layer

Let's consider a substrate material of height 'h', due to the addition of the first CS layer of height 'Δh', the stress increment distributes linearly in the substrate as:

$$\Delta\sigma_1(y) = a_1 y + b_1 \tag{A1}$$

The imposition of misfit strain due to the deposition of the first layer of deposited material generates a pair of equal and opposite forces in order to maintain an equilibrium condition. The equilibrium equation for the force in the x-direction for a unit width is given by:

$$\int_0^h \Delta\sigma_1(y)\, dy + \int_h^{h+\Delta h} k\, dy = 0 \tag{A2}$$

A pair of equal and opposite forces generate a bending moment; the equilibrium equation for the moment in the *x*-direction for a unit width is given by:

$$\int_0^h \{\Delta\sigma_1(y)\}\, y dy + \int_h^{h+\Delta h} (k)\, y dy = 0 \tag{A3}$$

Solving eq. (A2) and (A3):

$$a_1 = -\frac{6k\Delta h(h+\Delta h)}{h^3},\ b_1 = \frac{k\Delta h(2h+3\Delta h)}{h^2}$$

Therefore, from eq. (A1) the total stress increment in the substrate due to the addition of the first layer is given by:

$$\Delta\sigma_{TS_{(1L)}}(y) = \Delta\sigma_1(y) = -\frac{6k\Delta h(h+\Delta h)}{h^3}y + \frac{k\Delta h(2h+3\Delta h)}{h^2} \quad \text{(A4)}$$

(b) Deposition of the second layer

Let's consider, due to the addition of the second CS layer of height 'Δh', the stress increment distributes linearly in the substrate as:

$$\Delta\sigma_2(y) = a_2 y + b_2 \quad \text{(A5)}$$

The equilibrium equation for the force after the addition of the second layer in the *x*-direction for a unit width is given by:

$$\int_0^h \{\Delta\sigma_1(y) + \Delta\sigma_2(y)\}\,dy + \int_h^{h+\Delta h}\{k + \Delta\sigma_2(y)\}\,dy \; + \; \int_{h+\Delta h}^{h+2\Delta h}(k)\,dy = 0 \quad \text{(A6)}$$

The equilibrium equation for the moment after the addition of the second layer in the *x*-direction for a unit width is given by:

$$\int_0^h \{\Delta\sigma_1(y) + \Delta\sigma_2(y)\}\,ydy + \int_h^{h+\Delta h}\{k + \Delta\sigma_2(y)\}\,ydy \; + \; \int_{h+\Delta h}^{h+2\Delta h}(k)\,ydy = 0 \quad \text{(A7)}$$

Solving eq. (A6) and (A7):

$$a_2 = -\frac{6k\Delta h(h+2\Delta h)}{(h+\Delta h)^3},\; b_2 = \frac{k\Delta h(2h+5\Delta h)}{(h+\Delta h)^2}$$

Then, from eq. (A5) the stress increment due to the addition of the second layer is given by:

$$\Delta\sigma_2(y) = -\frac{6k\Delta h(h+2\Delta h)}{(h+\Delta h)^3}y + \frac{k\Delta h(2h+5\Delta h)}{(h+\Delta h)^2} \quad \text{(A8)}$$

So, the total stress increment in the substrate due to the addition of two layers is given by:

$$\Delta\sigma_{TS_{(2L)}}(y) = \Delta\sigma_1(y) + \Delta\sigma_2(y)$$

$$\Rightarrow \Delta\sigma_{TS_{(2L)}}(y) = -6ky\Delta h\left\{\frac{h+\Delta h}{h^3} + \frac{h+2\Delta h}{(h+\Delta h)^3}\right\} + k\Delta h\left\{\frac{2h+3\Delta h}{h^2} + \frac{2h+5\Delta h}{(h+\Delta h)^2}\right\} \quad \text{(A9)}$$

The total stress increment in the first layer due to the addition of the second layer is given by:

$$\Delta\sigma_{TL1_{(L2)}}(y) = k + \Delta\sigma_2(y)$$

$$\Rightarrow \Delta\sigma_{TL1_{(L2)}}(y) = k - \frac{6k\Delta h(h+2\Delta h)}{(h+\Delta h)^3}y + \frac{k\Delta h(2h+5\Delta h)}{(h+\Delta h)^2} \quad \text{(A10)}$$

(c) Deposition of the n^{th} layer

Let's consider, due to the addition of the n^{th} CS layer of height 'Δh', the stress increment distributes linearly in the substrate as:

$$\Delta\sigma_n(y) = a_n y + b_n \quad \text{(A11)}$$

The equilibrium equation for the force after the addition of the n^{th} layer in the *x*-direction for a unit width is given below:

$$= \left[\left\{\int_0^h \{\Delta\sigma_1(y) + \Delta\sigma_2(y) \dots\dots + \Delta\sigma_n(y)\}\,dy\right\} + \left\{\int_h^{h+\Delta h}\{k + \Delta\sigma_2(y) + \Delta\sigma_3(y) \dots\dots \Delta\sigma_n(y)\}\,dy\right\} + \left\{\int_{h+\Delta h}^{h+2\Delta h}\{k + \Delta\sigma_3(y) + \Delta\sigma_4(y) \dots\dots + \Delta\sigma_n(y)\}\,dy\right\} \dots\dots + \left\{\int_{h+(n-1)\Delta h}^{h+(n-2)\Delta h}\{k + \Delta\sigma_n(y)\}\,dy\right\} + \left\{\int_{h+(n-1)\Delta h}^{h+n\Delta h}(k)\,dy\right\}\right] = 0 \quad \text{(A12)}$$

The equilibrium equation for the moment after the addition of the n^{th} layer in the *x*-direction for a unit width is given below:

$$= \left[\left\{\int_0^h \{\Delta\sigma_1(y) + \Delta\sigma_2(y) \dots\dots + \Delta\sigma_n(y)\} y\, dy\right\} + \left\{\int_h^{h+\Delta h} \{k + \Delta\sigma_2(y) + \Delta\sigma_3(y) \dots\dots \Delta\sigma_n(y)\} y\, dy\right\} + \left\{\int_{h+\Delta h}^{h+2\Delta h} \{k + \Delta\sigma_3(y) + \Delta\sigma_4(y) \dots\dots + \Delta\sigma_n(y)\} y\, dy\right\} \dots\dots + \left\{\int_{h+(n-2)\Delta h}^{h+(n-1)\Delta h} \{k + \Delta\sigma_n(y)\} y\, dy\right\} + \left\{\int_{h+(n-1)\Delta h}^{h+n\Delta h} (k)\, y dy\right\}\right] = 0 \quad \text{(A13)}$$

Solving eq. (A12) and (A13):

$$a_n = -\frac{6k\Delta h(h+n\Delta h)}{\{h+(n-1)\Delta h\}^3},\ b_n = \frac{k\Delta h\{2h+(2n+1)\Delta h\}}{\{h+(n-1)\Delta h\}^2}$$

Therefore, from eq. (A11) the stress increment in the substrate due to the addition of the n^{th} layer is given by:

$$\Delta\sigma_n(y) = -\frac{6k\Delta h(h+n\Delta h)}{\{h+(n-1)\Delta h\}^3} y + \frac{k\Delta h\{2h+(2n+1)\Delta h\}}{\{h+(n-1)\Delta h\}^2} \quad \text{(A14)}$$

So, the total stress increment in the substrate due to the addition of 'n' layers is given by:

$$\Delta\sigma_{TS_{(nL)}}(y) = \Delta\sigma_1(y) + \Delta\sigma_2(y) + \Delta\sigma_3(y) \dots\dots\dots\dots + \Delta\sigma_{n-1}(y) + \Delta\sigma_n(y)$$

$$\Rightarrow \Delta\sigma_{TS_{(nL)}}(y) = -6ky\Delta h\left\{\frac{h+\Delta h}{h^3} + \frac{h+2\Delta h}{(h+\Delta h)^3} + \frac{h+3\Delta h}{(h+2\Delta h)^3} \dots\dots\dots + \frac{h+n\Delta h}{\{h+(n-1)\Delta h\}^3}\right\} + k\Delta h\left\{\frac{2h+3\Delta h}{h^2} + \frac{2h+5\Delta h}{(h+\Delta h)^2} + \frac{2h+7\Delta h}{(h+2\Delta h)^2} \dots\dots\dots + \frac{2h+(2n+1)\Delta h}{\{h+(n-1)\Delta h\}^2}\right\}$$

$$\Rightarrow \Delta\sigma_{TS(nL)}(y) = -6ky\Delta h\sum_{n=1}^{n}\left\{\frac{h+n\Delta h}{\{h+(n-1)\Delta h\}^3}\right\} + k\Delta h\sum_{n=1}^{n}\left\{\frac{2h+(2n+1)\Delta h}{\{h+(n-1)\Delta h\}^2}\right\} \quad \text{(A15)}$$

The total stress increment in the first layer due to the addition of the n^{th} layer is given by:

$$\Delta\sigma_{TL1_{(Ln)}}(y) = k + \Delta\sigma_2(y) + \Delta\sigma_3(y) \dots\dots\dots\dots + \Delta\sigma_{n-1}(y) + \Delta\sigma_n(y)$$

$$\Rightarrow \Delta\sigma_{TL1_{(Ln)}}(y) = k - 6ky\Delta h\left\{\frac{h+2\Delta h}{(h+\Delta h)^3} + \frac{h+3\Delta h}{(h+2\Delta h)^3} \dots\dots\dots + \frac{h+n\Delta h}{\{h+(n-1)\Delta h\}^3}\right\} + k\Delta h\left\{\frac{2h+5\Delta h}{(h+\Delta h)^2} + \frac{2h+7\Delta h}{(h+2\Delta h)^2} \dots\dots\dots + \frac{2h+(2n+1)\Delta h}{\{h+(n-1)\Delta h\}^2}\right\} \quad \text{(A16)}$$

The total stress increment in the second layer due to the addition of the n^{th} layer is given by:

$$\Delta\sigma_{TL2_{(Ln)}}(y) = \{k + \Delta\sigma_3(y) + \Delta\sigma_4(y) \dots\dots\dots\dots + \Delta\sigma_{n-1}(y) + \Delta\sigma_n(y)\}$$

$$\Rightarrow \Delta\sigma_{TL2_{(Ln)}}(y) = k - 6ky\Delta h\left\{\frac{h+3\Delta h}{(h+2\Delta h)^3} + \frac{t+4\Delta t}{(t+3\Delta t)^3} \dots\dots\dots + \frac{h+n\Delta h}{\{h+(n-1)\Delta h\}^3}\right\} + k\Delta h\left\{\frac{2h+7\Delta h}{(h+2\Delta h)^2} + \frac{2h+9\Delta h}{(h+3\Delta h)^2} \dots\dots\dots + \frac{2h+(2n+1)\Delta h}{\{h+(n-1)\Delta h\}^2}\right\} \quad \text{(A17)}$$

Total stress increment in the $(n-1)^{th}$ layer due to the addition of the n^{th} layer-

$$\Delta\sigma_{T\{L(n-1)\}_{(Ln)}}(y) = k + \Delta\sigma_n(y)$$

$$\Rightarrow \Delta\sigma_{T\{L(n-1)\}_{(Ln)}}(y) = k - \frac{6k\Delta h(h+n\Delta h)}{\{h+(n-1)\Delta h\}^3} y + \frac{k\Delta h\{2h+(2n+1)\Delta h\}}{\{h+(n-1)\Delta h\}^2} \quad \text{(A18)}$$

In order to write these equations (A16, A17, A18) in more simplified form, it can be assumed that there are m layers below the n^{th} layer; where, $m = 1, 2, 3, 4, \dots\dots\dots (n-1)$. For example: if $n = 7$, $m = 1, 2, 3, 4, 5, 6$

Therefore, the total stress increment in the $1^{st}, 2^{nd}, 3^{rd}, \ldots\ldots (n-1)^{th}$ layer respectively due to the addition of the n^{th} layer is:

$$\therefore \Delta\sigma_{T(Lm)_{(Ln)}}(y) = k - 6ky\Delta h \sum_{m+1}^{n} \left\{\frac{h+n\Delta h}{\{h+(n-1)\Delta h\}^3}\right\} + k\Delta h \sum_{m+1}^{n} \left\{\frac{2h+(2n+1)\Delta h}{\{h+(n-1)\Delta h\}^2}\right\} \quad \text{(A19)}$$

By using equation (A19), the stress increment in each layer needs to be calculated individually up to m layers by keeping the value of n constant. For example, if $n = 3$, $m = 1, 2$. Then, due to the addition of a 3rd layer, the total stress increment in the 1st layer needs to be calculated by using the value of $n = 3$ and $m = 1$ in equation (A19); similarly, the total stress increment in the 2nd layer needs to be calculated using the value of $n = 3$ and $m = 2$.

II. Mathematical derivations for thermal mismatch dominant cold spray process

Mathematical derivations for the thermal mismatch dominant CS process is very similar to that of the peening dominant CS process, which has been demonstrated in Appendix I.

III. Additional '*k*' values and other geometrical parameters

In addition to Table 1, a collated data set with measured '*k*' values and other geometrical variables from the literature are presented in Table A1, which can be used to validate the proposed analytical model.

Table A1: Additional information on measured '*k*' values and other geometrical parameters from the published literature.

Cases	Substrate/deposits	Assumed '*k*' value (MPa)	Substrate height '*h*' (mm)	Assumed layer height '*Δh*' (μm)	Number of layers '*n*'
(a)	KM Al/Mg (He, 132 °C) [6]	-11.94	3.4	230	20
(b)	KM Al/Mg (He; 77 °C) [6]	-15.58	3.4	230	20
(c)	KM Al/Mg (N_2; 217 °C) [6]	-13.74	3.4	185	20
(d)	CGT Ti/Cu [21]	48.50	3.0	235	20